Motion Correction for Perfusion Weighted Images in Stroke: Approach and Impact on Quantification

R. Mullick[1], D. Shanbhag[1], U. Patil[1], and X. Tao[2]

[1]Imaging Technologies Lab, GE Research, Bangalore, Karnataka, India, [2]Imaging Technologies Lab, GE Research, Niskayuna, NY, United States

Introduction: Head motion while imaging stroke, neoplasic and neuro-degenerative disease is often observed during routine clinical imaging [1]. Even with head stabilization, involuntary head movement can cause image artifacts leading to incorrect diagnosis. These artifacts have acute effects in select (extended duration) image sequences targeted to acquire spatio-temporal data like perfusion-weighted imaging and functional imaging scans. It is therefore imperative to address motion artifacts either early in the imaging chain or through a post-processing step. In cases of acute stroke, where time to image is of utmost importance, the extended duration of scan due to use of navigators precludes their use and places more importance on retrospective motion correction through image segmentation/registration techniques. In this work we present an approach based on image registration to align the spatio-temporal data, evaluate the impact on quantification of stroke related perfusion maps. The underlying challenge to correct and evaluate motion artifacts is further discussed.

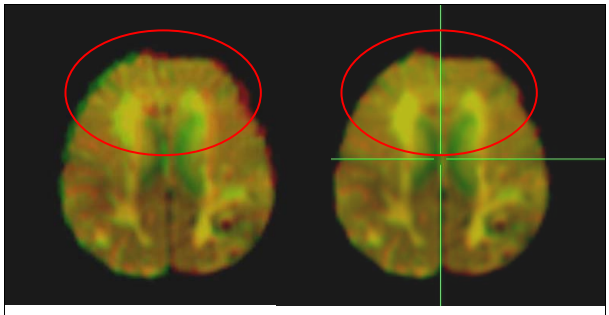

Figure 1: (Left) Overlay image of t=TR and t=5*TR (Before motion correction) and (Right) After motion correction using method (iv) SC+MC+SC. The red oval marks the region of visible corrections.

Methods: We evaluated our approach on acute stroke cases imaged on a 1.5T scanner (Signa Excite, GE Healthcare, Chalfont St. Giles, U.K.), using echo-planar 2D PWI with TR/TE =2000/60, 128x128 matrix. 20 Sections (6mm thick, 1mm gap), acquired to ensure full head coverage with a FOV of 25cm and 30 phases. The multi-phase data was acquired during the bolus injection of gadolinium-based contrast agent. Our approach to arrest motion, distinct from prior efforts [2-5], incorporates 3D symmetry correction to compliment a 3D image registration step, between the reference (1st time point) and all consecutive gates. This is motivated by the fact that typical head movement would be a 3D rotation/translation and could not be restricted to within a 2D plane. Symmetry correction [6] is based on deriving a transform between the original single phase data and a mirror image of the same. The evaluated approach for motion correction has 4 main steps: (1) Reformation of the temporal raw signal data into multi-phase 3D volumes; (2) Application of a symmetry correction step to ensure the data is always represented in standard space with the mid-sagittal plane falling in the middle of the volume; (3) Gradient descent optimization of an affine transform with respect to a Normalized Correlation Coefficient metric of the reference image (t=TR) and all phases thereafter; (4) Tri-linear interpolation of the phase data based on the optimum transform. The symmetry correction and registration algorithms were implemented using functionality available in the Insight Toolkit (ITK) [7].

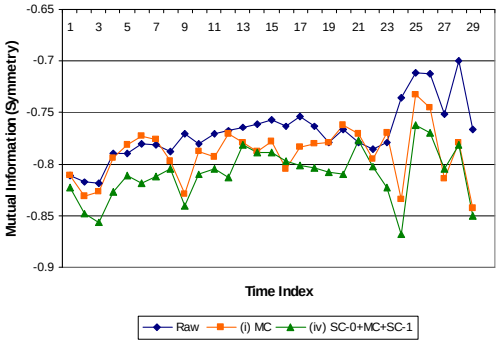

Figure 2: Mutual Information metric with respect to symmetry axis within each phase point. Closer the phase volume is to its symmetry axis, lower is the MI metric and more uniform is the alignment.

Results & Discussion: Two (n=2 of 13) PWI datasets with varying degree of head motion were included as part of this evaluation. Optimum visual analysis is only possible by animating through the phases, so here we attempt to illustrate the results under static display constraints. Five unique runs were compared to the original raw perfusion data: (i) Motion Correction (MC); (ii) Symmetry Correction (SC); (iii) SC+MC; (iv) SC+MC+SC; and (v) MC+SC. Figure 1 shows an red-green overlay view of the motion mismatch before and after the correction (Case 0022, Run 4, Ph. 1 & 5). In Figure 2, we plot the aggregate improvement in each phase as measured by the degree of L-R hemispherical symmetry using Mutual-Information (Lower the MI value the more aligned the data). Notice the near-consistent Lower MI (better match) value for the processed data (iv) SC-0+MC+SC-1 compared to the raw signal. Figure 3 graphs the signal intensity curves before and after the motion correction for a point in near the mid-sagittal plane. The impact on quantitative assessment is depicted in Figure 4 showing the absolute change in the measured MTT Value before and after motion correction for the same axial section as in Figure 1.

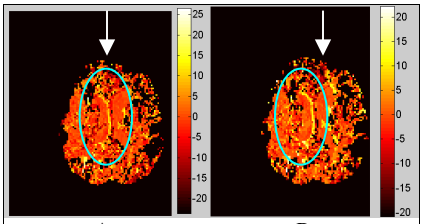

Figure 4: The difference in MTT as observed between the original motion corrupted dataset and (A) MC only scheme and (B) SC+MC+SC scheme. Notice that figure B also has better alignment to symmetry axis (white arrow and observing the CSF residuals (rings))

Conclusion & Future Directions: The work demonstrates the need and potential correction of motion artifacts, and possible impact on the quantification of time varying MR signal data. Motion will lead to inaccuracies in computation of the lesion volume, tumor margins, neoangiogenesis, and special localization of functional data. The lack of sharp features in the images makes the evaluation task very difficult. An objective evaluation based on clinical inputs is a possibility. Furthermore, the EP distortion in anterior and posterior brain regions and the presence of image ghosts due to limited acquisition time can further detract the correction algorithm. The authors are also evaluating the efficacy of incorporating a whole brain mask based algorithm to further enhance the results by eliminating ghost images as marked in Figure 3A (red arrow).

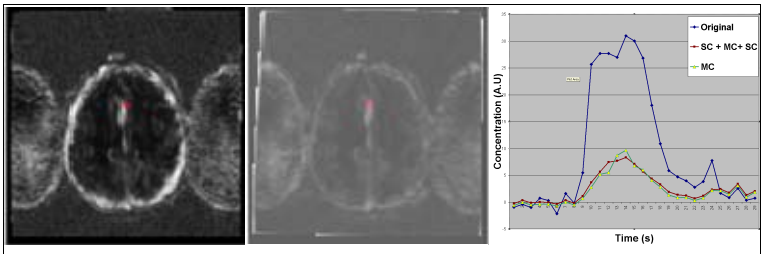

Figure 3:(A) shows the raw data which was corrupted with motion, while (B) shows the data corrected with scheme: (iv) SC+MC+SC. The yellow arrow clearly shows the corrections done by the scheme to freeze motion and bring all phases in same alignment in 3D. (C) shows how the motion freezing can vastly change the concentration curve profile at a particular location.

References:

[1] Quantitative MRI of the Brain, Paul Tofts, Wiley, 2003.
[2] CATNAP/VIPAR: http://iacl.ece.jhu.edu/resources/
[3] MCFLIRT: http://www.fmrib.ox.ac.uk/fsl/mcflirt/;
[4] NeuroImage 17, 825–841, 2002;
[5] JMRI;26:1167–1172, 2007.
[6] X. Tao & S. Gupta, ISMRM 2009 (Abstract Submitted);
[7] http://www.itk.org